

# Chapter 2

## Optical Waveguide

In this chapter, the fundamental theory from Maxwell's equations and the propagation of light in the optical waveguide is discussed. Several equations were used to describe the electromagnetic waves guide. We explain common design methods and the analysis of the optical waveguide by Finite Difference Time Domain Method (FDTD). The region of optical waveguide is divided into smaller elements. By calculating the correlating matrices from the smaller elements, we can image how light-wave propagates in the optical waveguide. In section 2-3, we discuss about the sidewall's roughness and the discontinuities in an optical waveguide. In section 2-4, we simulate the results of those roughness and discontinuities in optical waveguides. Finally the technical information and references on the simulation methods used in Full-WAVE are given [61].

## 2-1 Basic Theory of Wave Propagation in Waveguide

Light wave is characterized by a combination of a time-varying electric and magnetic fields that are propagating, so they can be described by the four Maxwell wave equations [27-31]. Maxwell showed that both these fields satisfy the same partial differential equation which is called wave equation as shown below [33]:

$$\nabla^2(\vec{E}, \vec{H}) = \frac{1}{c} + \frac{\partial^2}{\partial t^2}(\vec{E}, \vec{H}) \quad (2-1)$$

where  $\vec{E}$  and  $\vec{H}$  are the electric and magnetic fields. These fields are frequently displayed in component form by means of matrix representation, with  $E_x$ ,  $E_y$  and  $E_z$ , where  $c$  is the speed of light that propagates through the fields. Therefore, the wave equation for the electric field in vacuum is:

$$\nabla^2 \vec{E} = \frac{1}{c} + \frac{\partial^2}{\partial t^2} \vec{E} \quad (2-2)$$

The solution to the equation (2-2) has the following general form:

$$\vec{E}(x, y, z, t) = a_+ \vec{E}^+(\vec{k} \cdot \vec{r} - \omega t) + a_- \vec{E}^-(\vec{k} \cdot \vec{r} + \omega t) \quad (2-3)$$

where  $\vec{r} = (x, y, z)$  is the position vector,  $\vec{k} = (k_x, k_y, k_z)$  is the wave

propagation vector, and  $\omega$  is the angular frequency.

Waveguides are structures within the electromagnetic waves that guide the light-wave propagation. There are many different kinds of waveguides that can be generally divided into two important categories: rectangular and circular. Many physical concepts are the same in different kinds of waveguides, such as boundary conditions and propagation modes. Here we will solve wave equations of waveguide propagation for a rectangular waveguide.

If we let  $Z$  be the longitudinal direction of the waveguide along which a wave propagates. The electric and magnetic fields can be expressed as

$$\bar{E}(x, y, z, t) = E(x, y)e^{j(\omega t - \beta_z z)} \quad (2-4)$$

$$\bar{H}(x, y, z, t) = H(x, y)e^{j(\omega t - \beta_z z)} \quad (2-5)$$

where  $E(x, y)$  and  $H(x, y)$  are the transverse factors of the corresponding fields,  $e^{j(\omega t - \beta_z z)}$  is the common longitudinal factor and  $\beta$  is called a propagation constant. Assuming that there is no magnetic field component in the  $Z$  direction (TM modes),

$$H_z = 0 \quad (2-6)$$

The solutions are separated into two waves: one that has only transverse and

no longitudinal magnetic field, that is,  $H_z=0$ ; and the other that has only transverse and no longitudinal electric field, that is,  $E_z=0$ . The former is called transverse magnetic or TM mode (wave) and the latter, a transverse electric or TE mode. In general, a wave has both  $H_z$  and  $E_z$  components. The  $H_z$  component is accounted for by the  $H_z$  component of the TE mode and the  $E_z$  component, by the  $E_z$  component of the TM mode. The field is composed of both TM and TE modes in general. Substituting the equations (2-4) and (2-5) into Maxwell's equations and assuming the current density is zero, we have:

$$E_x = -\frac{1}{\beta^2 - \beta_z^2} \left( A \frac{\partial E_z}{\partial x} + B \frac{\partial H_z}{\partial y} \right) \quad (2-7)$$

$$E_y = \frac{1}{\beta^2 - \beta_z^2} \left( -A \frac{\partial E_z}{\partial y} + B \frac{\partial H_z}{\partial x} \right) \quad (2-8)$$

$$H_x = \frac{1}{\beta^2 - \beta_z^2} \left( C \frac{\partial E_z}{\partial y} - D \frac{\partial H_z}{\partial x} \right) \quad (2-9)$$

$$H_y = -\frac{1}{\beta^2 - \beta_z^2} \left( C \frac{\partial E_z}{\partial x} + D \frac{\partial H_z}{\partial y} \right) \quad (2-10)$$

here  $A=j\beta_z$ ,  $B=j\omega\mu_0$ ,  $C=j\omega\epsilon$ ,  $D=j\beta_z$  and  $\beta=\omega \sqrt{\epsilon\mu_0} = \frac{n\omega}{c}$  is the propagation constant of the waveguide medium. Constants  $\epsilon$  and  $\mu_0$  are the vacuum permittivity and permeability. In addition to the equations (2-7) ~ (2-10),

electromagnetic waves that can propagate in a rectangular waveguide also need to fulfill certain boundary conditions. Waves that can satisfy both of the equations and conditions mentioned above are called propagation modes.

## **2-2 Common Analysis Methods for Optical Waveguide**

In this section, we will give the explanations of common design methods: Finite Element Method (FEM) [29-31, 36], Finite Difference Method (FDM) [31], Beam Propagation Method (BPM) [35], and Finite Difference Time-Domain Method (FD-TDM) [41].

The Finite Element Method is widely used for the analysis of the investigation in the propagation characteristics of any of the various arbitrarily shaped optical waveguides [30-32, 36]. The Finite Element Method can be used to solve optical waveguide problems by using the matrix eigenvalue equations. In the Finite Element Method, the region of interest is divided into the smaller elements. After the discretion model for each element is constructed, all the contributions from the elements are assembled into the system. We can drive the matrix elements in the eigenvalue equation and explain how their calculation can be programmed. The Finite Element Method is somewhat similar to the Finite Difference Method, and is widely used in the Computer Aided Design (CAD). Therefore, the Finite Difference Method is a more direct approach to solve the wave equations. Finite difference schemes are also used in the Finite Difference Beam Propagation Methods, which are also used in the CAD

software. Finite Difference Method drives the fully vectorial and semivectorial wave equations for the quasi-TE and quasi-TM modes. Beam Propagation Methods (BPMs), which is developed for the analysis of nonuniform waveguides such as bends and tapers. There are various kinds of BPMs that have been developed, such as the Fast Fourier Transform (FFT-BPM) [34], the Finite Difference (FD-BPM) [37], and the Finite Element (FE-BPM) [38]. Finite Difference Time-Domain Method directly solves the time dependent in the Maxwell equations. It was originally proposed for long wavelengths electromagnetic wave, but it is a little difficult to apply to 3D optical waveguides from the viewpoint of a computer.

## **2-3 Analysis of Optical Waveguide Fabrication Caused Defects**

Silicon on silicon dioxide wafer having a large refractive index difference which can induce high electromagnetic field confinement in the silicon guiding layer that in turn allows reducing the waveguide size to sub-micrometer values. With this benefit, Silicon-on-Insulator (SOI) wafer is broadly used in fabricating optical waveguide devices. The common fabrication for SOI waveguide uses a semiconductor process. Ideal SOI waveguide transmits with a low propagation loss. But, it is well known that for the technological limitations, the fabrication of waveguide will cause sidewall's roughness and discontinuities. In fact, there still exists many factors that will influence light waves broadcasted inside the waveguide. As shown in Fig. 2.2, we can see waveguides with the sidewall's roughness. The width of those rib waveguides is  $5.3\mu\text{m}$ , the slab height is  $5\mu\text{m}$  and the total rib height is  $6.7\mu\text{m}$ . In Fig. 2.3, there is a discontinuities region which may be caused by dust during lithography process. In this section, we will discuss the propagation loss caused by waveguide defects.

### **2-3-1 Sidewall's Roughness in Straight Waveguide**

The sidewall's roughness and discontinuities in an optical waveguide play important roles in designing optical components. The sidewall's roughness

leads to local variations of the effective index. Optic scattering at randomly rough surfaces are very difficult to exactly test at a plane waveguide. The Root-Mean-Square (RMS) roughness can range upward to 1.5% of the waveguide width [43]. Many studies report that the propagation loss calculations taking into account from roughness and also computationally solving with Beam Propagation Method (BPM) and Finite Difference Time-Domain Method (FDTD) [39-48]. To describe the manner in which these heights vary along a surface, those studies are often given in the form of a correlation function  $C_R$ , which corresponds to a measurement of the average correlation between one positions along the waveguide with another set at a distance  $d_w$ . Correlation function  $C_R$  described by an exponential correlation function is assumed in the following such as [39, 41, 46]

$$C_R \approx \zeta^2 e^{-\frac{|d_w|}{C_1}} \quad (2-11)$$

The Parameter  $\zeta$  here means the standard deviation of the perturbation function and  $C_1$  is the correlation length. The sidewall's roughness is described by a real space function  $F$ . Parameter  $\zeta$  is readily obtained by measuring the deviation of  $F$  from the linear mean of the sidewall.  $C_1$  is obtained from the autocorrelation function  $C_R$  of  $F$ . The scattering loss coefficient can be written as [39, 41, 46]

$$\alpha_r = \frac{\zeta^2}{k_0 \sqrt{2} d^4 n_1} GF \quad (2-12)$$

Function  $G$  is dependent on the waveguide geometry with the normalized frequency [46]. From the two equations above, we can immediately make a number of observations as to the dependence of the attenuation on the various waveguide parameters. Apart from the quadratic dependence of the coupling on the RMS roughness  $\zeta$ , exists a nontrivial dependence on the correlation length  $C_1$ .

## **2-4 Simulation of Discontinuities in Optical Waveguide**

### **2-4-1 Simulation of Waveguide Fabrication Caused Defects**

Now there will be a brief analysis of the optical waveguide fabrication that caused defects. Here, we will simulate the waveguide fabrication that caused defects. This section provides technical information and references on the simulation methods used in Full-WAVE [49]. The objective of Full-WAVE is to provide a general simulation package for computing the propagation of light waves in arbitrary waveguide geometries. The simulation is based on the well-known finite-difference time-domain (FDTD) technique. The physical propagation problem requires two key pieces of information:

1. The refractive index distribution,  $n(x,y,z)$ .
2. The electromagnetic field excitation.

From these, the physics dictates the electromagnetic field as a function of  $(x,y,z,t)$ .

In this section, we have designs of several rectangular waveguides with regular and irregular defects on the waveguide itself as the imperfection of the fabrication. The schematic diagrams of our optical waveguide are shown in Fig. 2.4. Extremely high refractive index contrast between the silicon core

( $n=3.5$ ) and silica cladding ( $n=1.5$ ). The specification of the waveguide is the width of  $5.3\mu\text{m}$  and length of  $50\mu\text{m}$  below the free space wavelength  $\lambda_c = 1.55\mu\text{m}$ . We put different kinds of rectangle, circle and ellipse waveguide on straight waveguide. Also we separate the simulation into the smaller imperfect sidewall's roughness and large fabricated defects of waveguide. However, the radiation modes have so far only been constructed in a relatively simple situation for two-dimensional (2-D) slab waveguides.

At first, we set the regular ellipse and trapezoid waveguides as a waveguide with the sidewall's roughness. Fig. 2.5 shows diagrams of our optical waveguides. There are three kinds of common sidewall roughness. One of them is the ellipse waveguides and others are trapezoid waveguides. From the Fig. 2.6, different results are also observed when the length of the two parallel sides are changed. As the length of the ellipse's major axis ( $R_a$ ) increases, the roughness attenuation increase as well. With the results of the simulation, it will be clear that the roughness attenuation of trapezoid waveguides are more serious than the ellipse waveguides.

Second, we put a large sized square, ellipse or circle on a straight waveguide as a large fabricated defect of waveguide which may be caused by dust during lithography process. Fig. 2.7 shows diagrams of our optical waveguides. From the Fig. 2.8 and Fig. 2.9, different results are also

observed when there is a change in the radius of circle ( $R$ ), as the length of the ellipse's major axis ( $R_a$ ) increases and so will the length of the square and the trapezoid ( $L$ ).

### **2-4-2 Simulation of a Regular Waveguide's Sidewall Defects**

From section 2-3-1, it is known that from correlation function and means standard deviation of the perturbation function, we can immediately make a number of observations as to the dependence of the attenuation on the various waveguide parameters. In this section, we will design a regular sidewall's roughness which can be approached to nearby waveguide width.

As Fig. 2.10 shows, we use circular form bullets to sculpture two straight lines on our wafer. These two straight lines will press from both sides of a straight waveguide. We can calculate the correlation function accurately from the geometric figure shown in Fig. 2.11. By varying the radius of the circular form bullets and change of the sculpture distance; we can get the waveguide with different widths. This advantage can be used in a fabricated waveguide without minding the propagation loss caused from perturbation to the roughness.

After a brief introduction of our design, we will show the result of a

simulation to fit our ideal waveguide. The waveguide as shown in Fig. 2.12, the refractive index contrasts between the silicon core ( $n=3.5$ ) and silica cladding ( $n=1.5$ ). The waveguide has length of  $50\mu\text{m}$  below the free space wavelength  $\lambda_C = 1.55\mu\text{m}$ . At first, we simulate a smooth waveguide as a reference value, and we change the waveguide width from  $4.02\mu\text{m}$  to  $4.1\mu\text{m}$ . Then we put our waveguide into simulation with regular sidewall's roughness. We tune the radius from  $10\mu\text{m}$  to  $20\mu\text{m}$  and distance of two center of a circle from  $1\mu\text{m}$  to  $2\mu\text{m}$ . The results of simulation are shown in Fig. 2.13. With comparison of the propagation loss shown in Fig. 2.13, we can get the correlation width from the results of the simulation. Through this correlation width, we can fabricate a waveguide device with better performance.

## **2-5 Summary**

Light-waves and electromagnetic waves can be described by the Maxwell wave equations. This chapter provides background about the wave propagation discussed in the various parts of the optical waveguide. It has also been discussed the situations in which there is a propagation loss from fabricated defects of waveguide. From the results of the simulation, the roughness attenuation of trapezoid waveguides are more serious than ellipse waveguides. And this result also fits in with the large size of fabricated defects on the waveguide, which may be caused by dust during the lithography process.

At last, we have designed a regular sidewall's roughness which can be approached to a nearby waveguide width. We have showed the result of the simulation to fit our ideal waveguide.

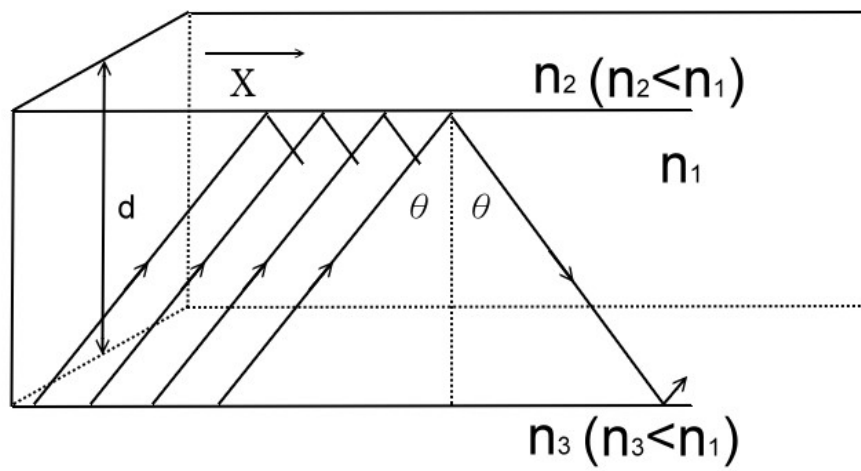


Fig. 2.1 Ray of light propagates in a planar waveguide.

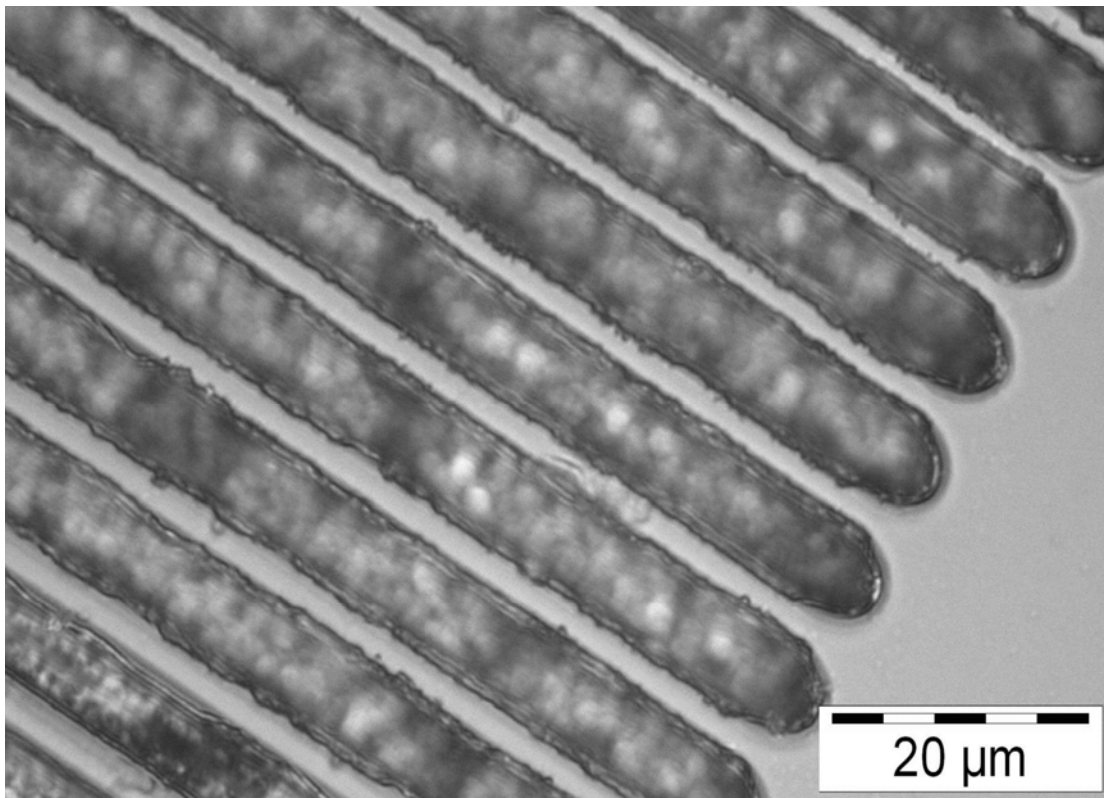


Fig. 2.2. Optical Waveguide Fabrication Caused Defects (1)

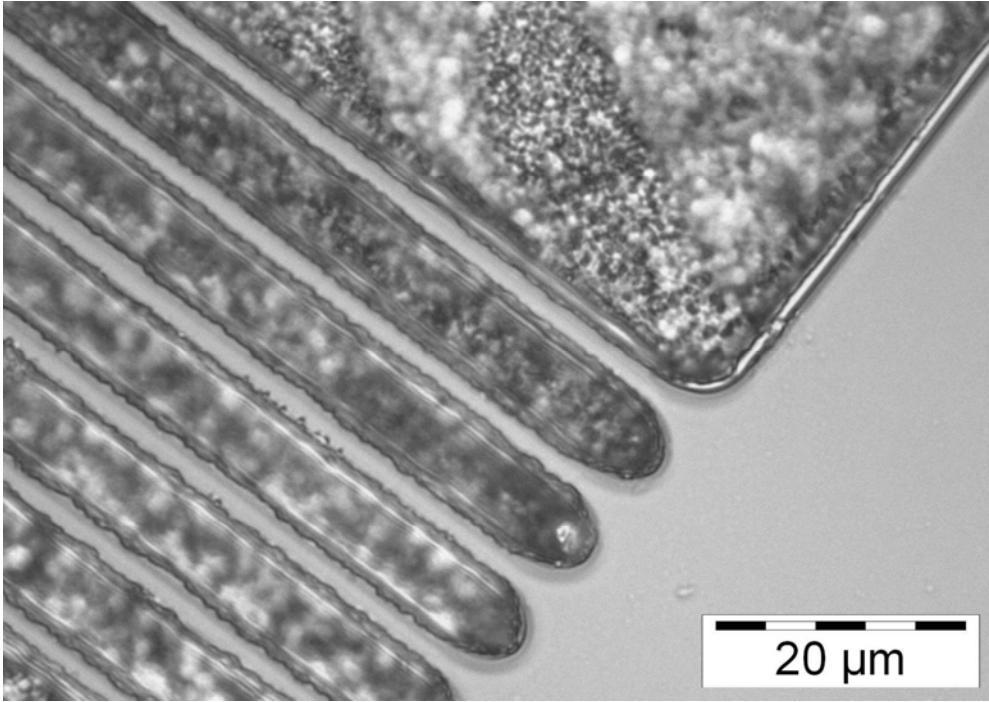


Fig. 2.3. Optical Waveguide Fabrication Caused Defects (2)

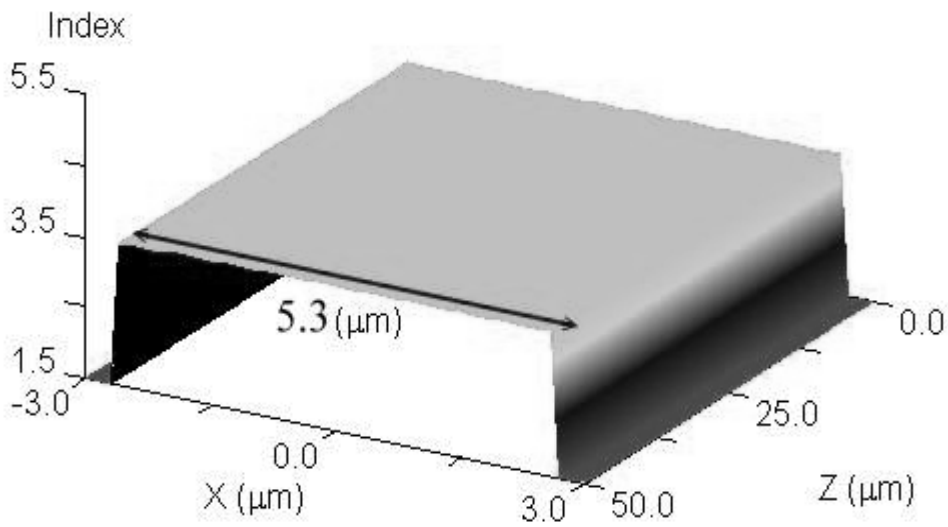


Fig. 2.4 The schematic diagrams of optical waveguide.

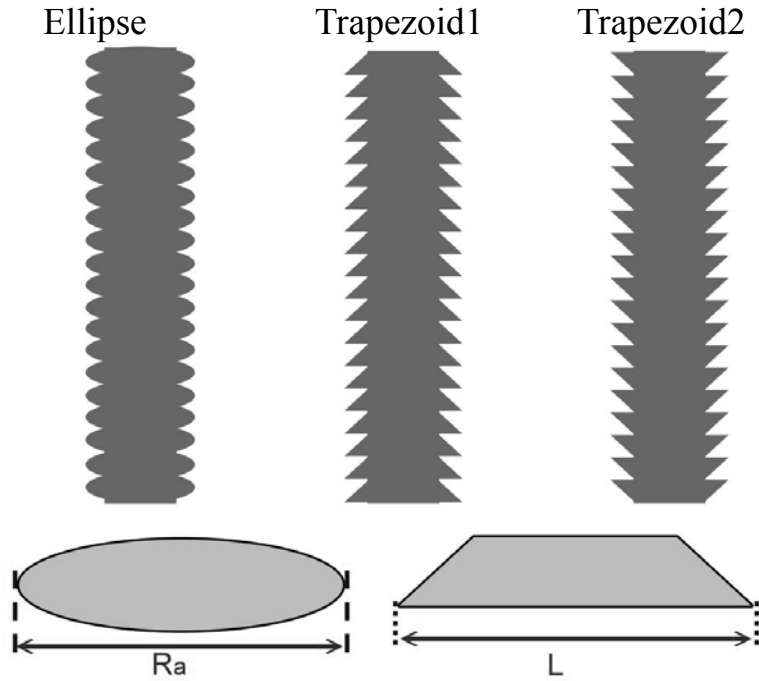


Fig. 2.5. Diagrams of simulation waveguides sidewall roughness

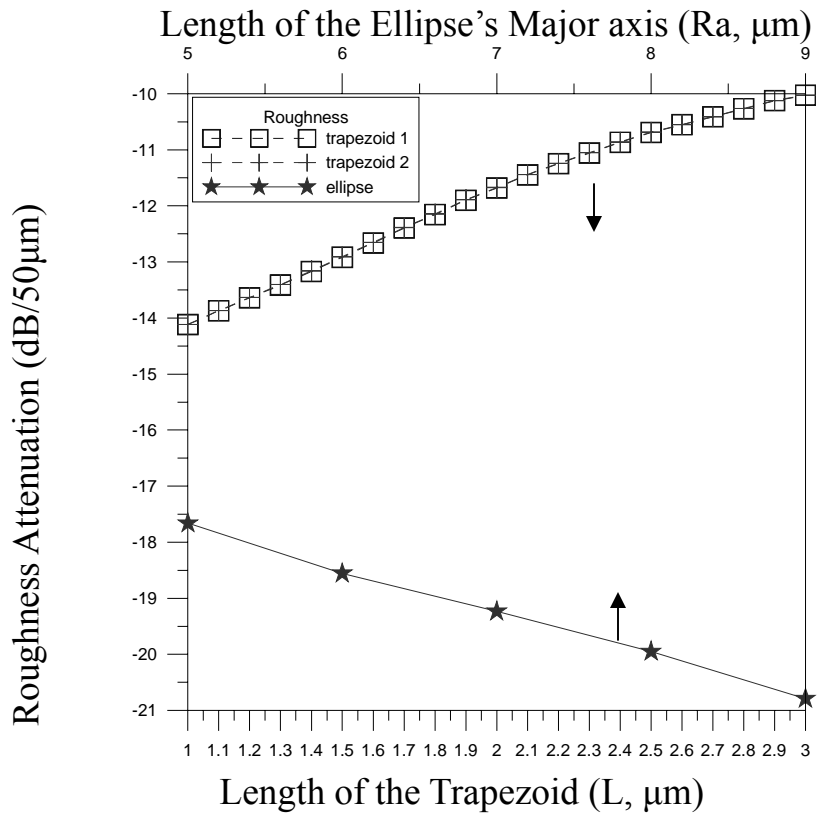


Fig. 2.6. Simulation results of sidewall roughness propagation loss

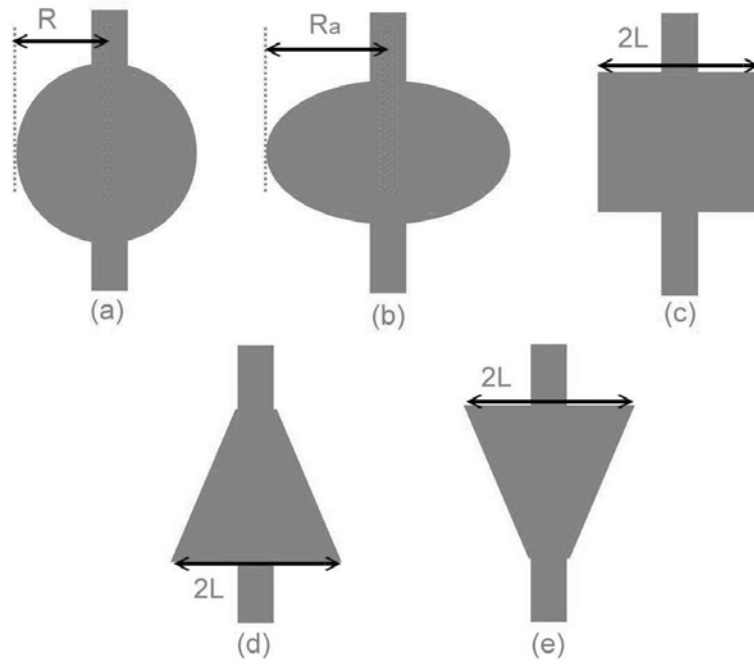


Fig. 2.7. Diagrams of fabricated defects of waveguides

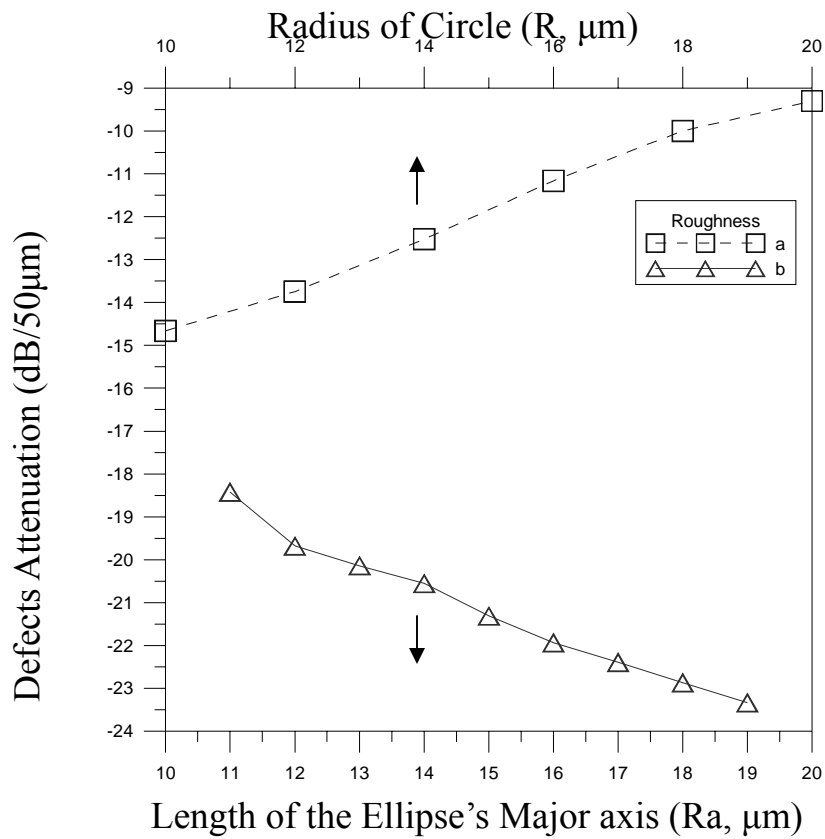


Fig. 2.8. Simulation results of circle and ellipse propagation loss

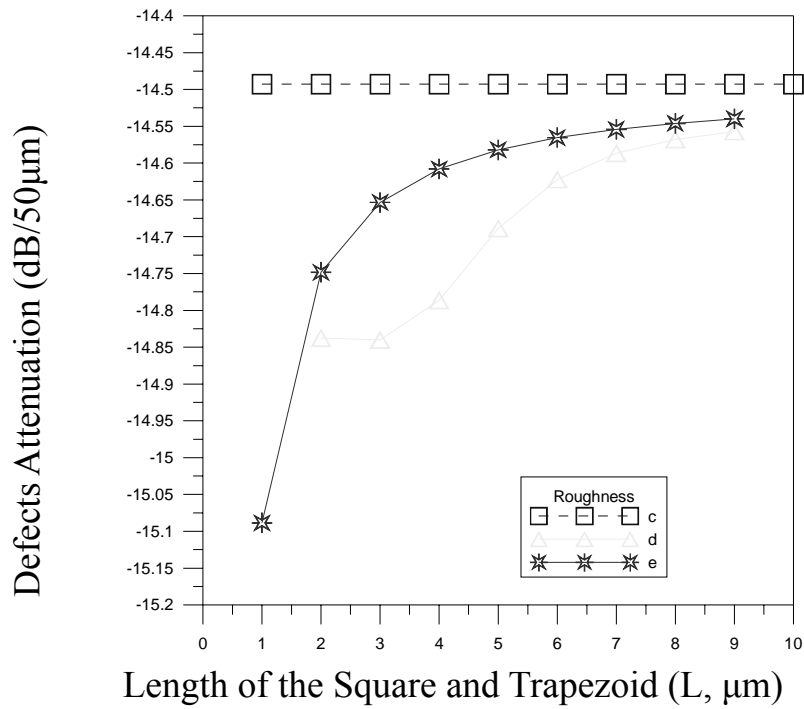


Fig. 2.9. Simulation results of square and trapezoid defects propagation loss

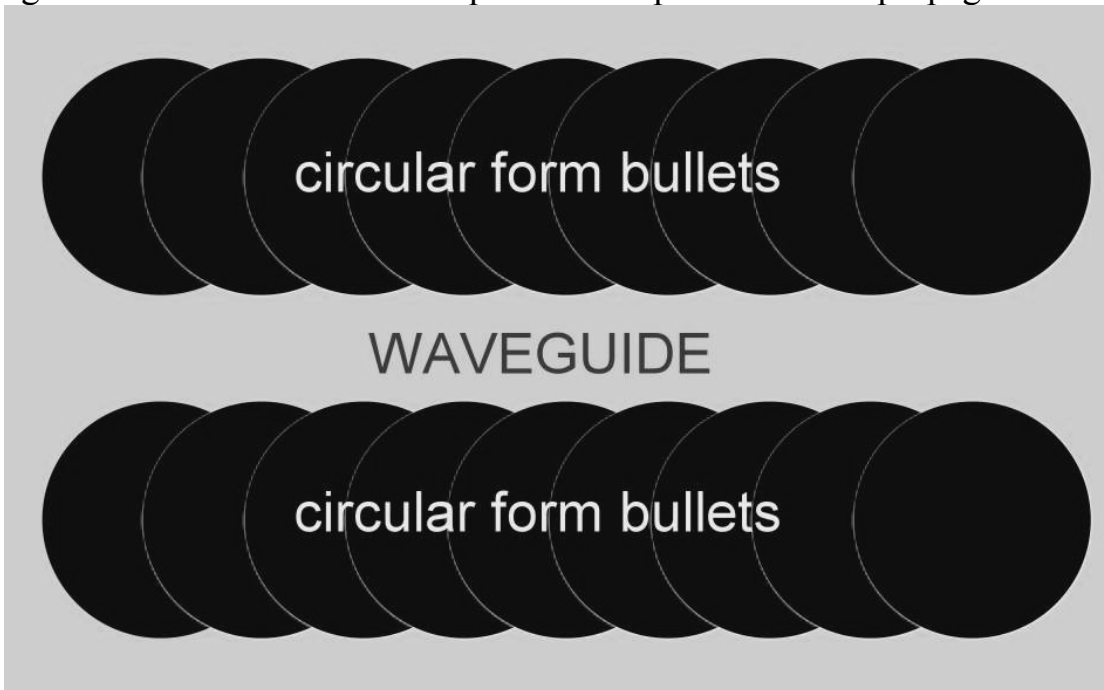


Fig. 2.10. Schematic diagram of regular sidewall's roughness waveguide.

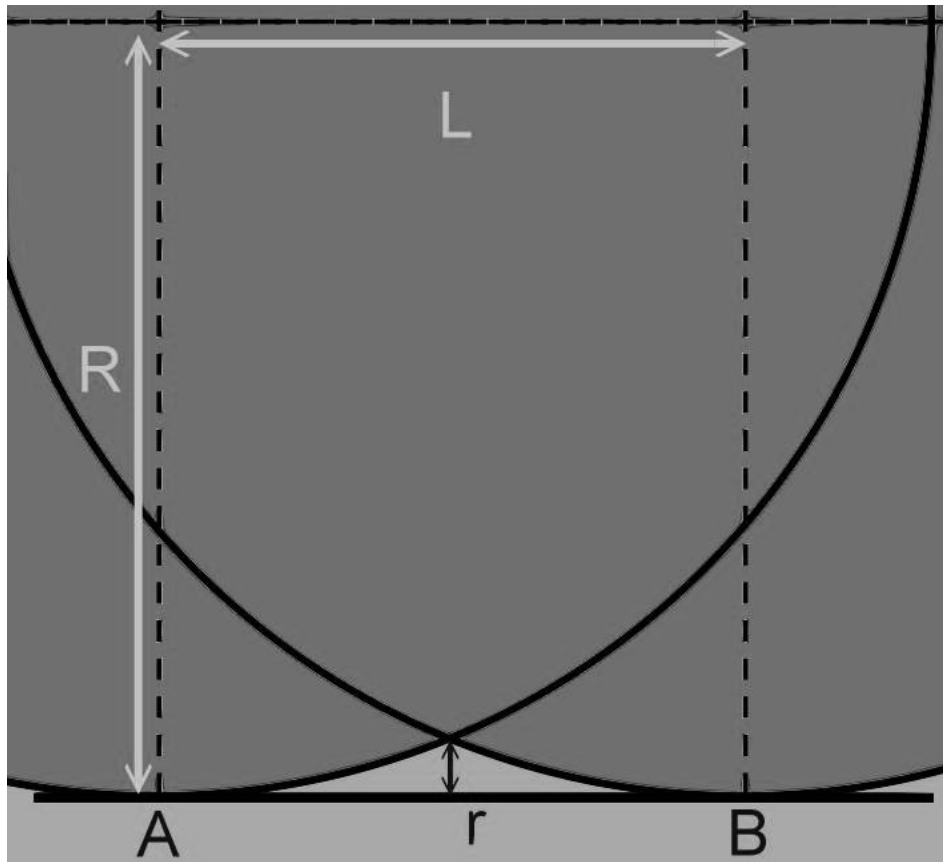


Fig. 2.11. Geometric figure of waveguide sidewall.

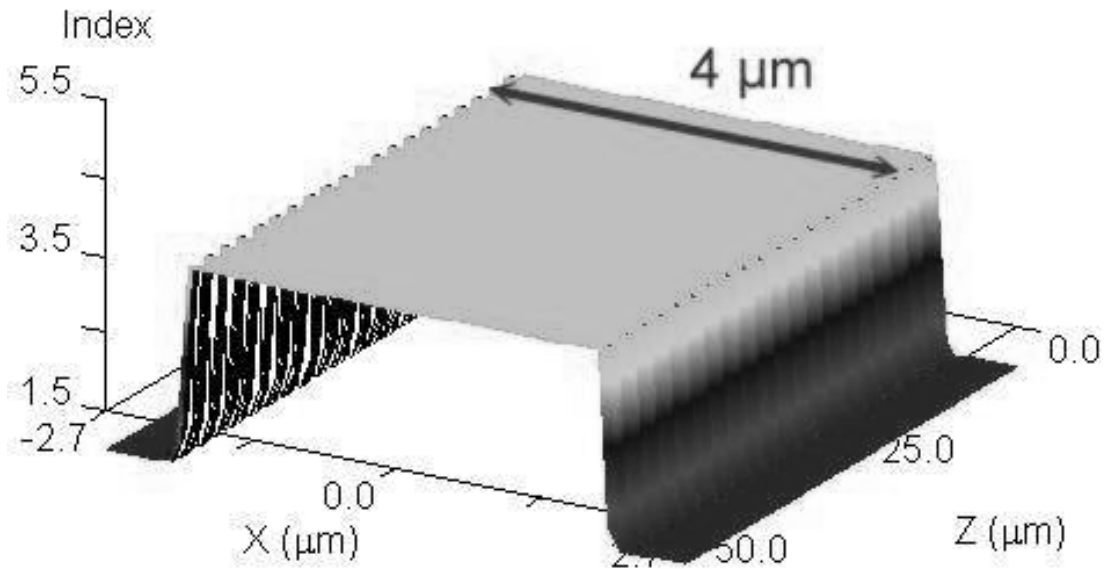


Fig. 2.12 The schematic diagrams of ideal optical waveguide with regular sidewall's roughness.

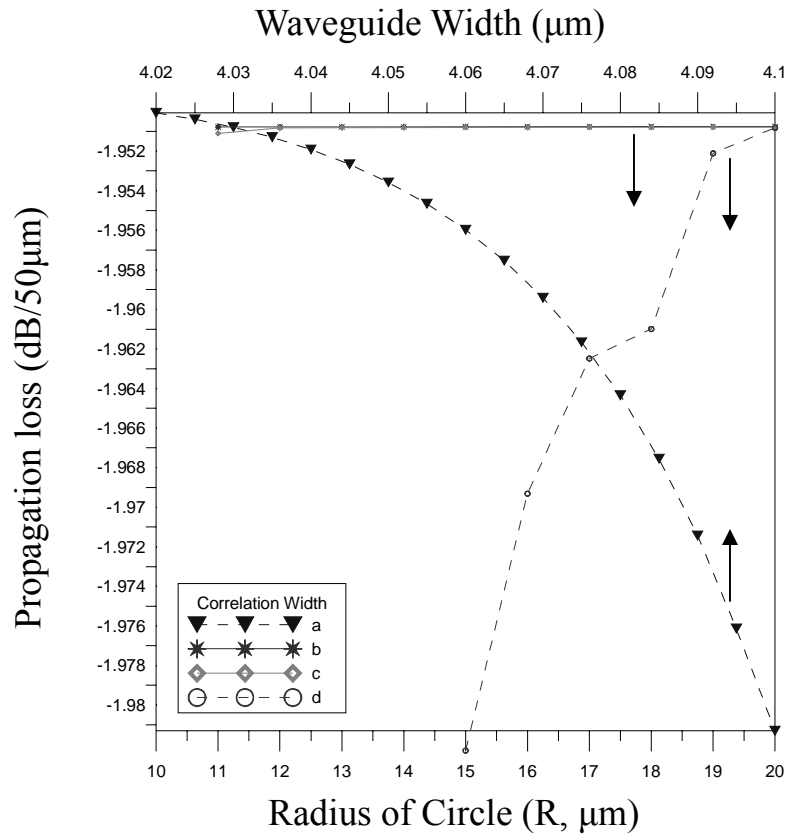


Fig. 2.13. Propagation of regular waveguide sidewall (a) smooth waveguide with change the width forms 4.02  $\mu\text{m}$  to 4.1  $\mu\text{m}$ . Comparison of regular waveguide's sidewall with vary radius and change the distance of center of circle (b)  $L=1\mu\text{m}$ , (c)  $L=1.5\mu\text{m}$  and (d)  $L=2\mu\text{m}$ .